

AN IN-HOST MODEL OF HIV INCORPORATING LATENT INFECTION AND VIRAL MUTATION

STEPHEN PANKAVICH

Department of Applied Mathematics and Statistics
 Colorado School of Mines
 Golden, CO 80401, USA

DEBORAH SHUTT

Department of Applied Mathematics and Statistics
 Colorado School of Mines
 Golden, CO 80401, USA

(Communicated by the associate editor name)

ABSTRACT. We construct a seven-component model of the in-host dynamics of the Human Immunodeficiency Virus Type-1 (i.e, HIV) that accounts for latent infection and the propensity of viral mutation. A dynamical analysis is conducted and a theorem is presented which characterizes the long time behavior of the model. Finally, we study the effects of an antiretroviral drug and treatment implications.

1. Introduction and Model. The human immune system is a complex network of interacting cells, cell products, and cell-forming tissues that protects the body from pathogens, destroys infected and malignant cells, and removes cellular debris [11]. A key component of this system is the white blood cell known as a T cell. In particular, the $CD4^+$ T cell moves throughout the body, identifying bacteria and viruses and directing the immune system's attack. Within healthy individuals the blood concentration of these cells is relatively constant, around 10^6 cells/ml [5]. HIV molecularly recognizes $CD4^+T$ cells as compatible for viral replication. As HIV is a retrovirus, it replicates within a host via reverse transcription using its RNA and an enzyme (reverse transcriptase) to create a strand of HIV DNA, called a provirus, which carries its genetic information. Once the provirus is created within a $CD4^+T$ cell, its immunological function ceases and it is used to create new virions [1]. Interestingly, reverse transcription is quite error prone, and the probability of mutation is high (around 22% of infected cells carry proviral genomes with at least one mutation [8]). Without being activated by antigens, an infected $CD4^+T$ cell, containing a provirus, fails to produce

2010 *Mathematics Subject Classification.* Primary: 37N25, 92B05; Secondary: 34D20.

Key words and phrases. HIV, in-host dynamics, latent infection, viral mutation, ART.
 This work is supported by National Science Foundation grant DMS-1211667.

new virus particles. In such a case, the T cell is referred to as latently infected [2, 9, 10].

The following model describes interactions between T cells and the populations of a wild-type and mutation of HIV. It incorporates latent infection of T cells and accounts for a single mutation within the virus. Specifically, the model is comprised of seven nonlinear ODEs given by

$$\left. \begin{aligned} \frac{dT}{dt} &= \lambda - d_T T - k_s TV_s - k_r TV_r \\ \frac{dI_s}{dt} &= (1-p)(1-\mu)k_s TV_s + \alpha_s L_s - d_I I_s \\ \frac{dL_s}{dt} &= p(1-\mu)k_s TV_s - \alpha_s L_s - d_L L_s \\ \frac{dV_s}{dt} &= N_s d_I I_s - d_V V_s \\ \frac{dI_r}{dt} &= (1-p)\mu k_s TV_s + (1-p)k_r TV_r + \alpha_r L_r - d_I I_r \\ \frac{dL_r}{dt} &= p\mu k_s TV_s + p k_r TV_r - \alpha_r L_r - d_L L_r \\ \frac{dV_r}{dt} &= N_r d_I I_r - d_V V_r. \end{aligned} \right\} \quad (7CM)$$

Here T denotes the population of healthy T cells whose maturity rate is λ and death rate is d_T . The parameter k_s is the rate of infection by the wild-type virus, whose population is denoted by V_s . Note that the T cells infected by the original strain, $k_s TV_s$, contribute to several other populations. I_s and L_s denote the populations of wild-type actively or latently infected T cells, respectively. The proportion of T cells which become latently infected is given by p . I_r and L_r are the populations of T cells that are actively and latently infected by the mutated strain, while the mutation rate of the wild-type virus is $\mu \in [0, 1]$. Note that T cells which are infected by the wild-type strain may create a mutated provirus and thus the terms $(1-p)\mu k_s TV_s$ and $p\mu k_s TV_s$ are included. The activation rates of latently infected cells to actively infected are α_s and α_r for the wild-type and mutated strains. The death rates of actively and latently infected T cells, regardless of strain, are d_I and d_L . N_s and N_r are the numbers of virions (wild and mutated) released by an infected T cell over its lifespan. Finally, d_V is the viral clearance rate for both strains. See the review [6] for more information. Parameter values are in Table 1, while Fig. 1 presents a simulation of (7CM) with this data. Both strains persist in the simulation, but the wild-type dominates the mutated strain by five orders of magnitude. In subsequent sections we will utilize analytic and computational methods to study (7CM) and discuss the effects of antiretroviral drugs on these populations.

2. Analysis and Dynamics. With the model finalized, we turn to an analysis of its behavior. First, well-posedness of solutions to (7CM) can be shown using the Picard-Lindelöf Theorem and known *a priori* bounds. The details are standard so we omit them. Instead, we focus on the asymptotic behavior

TABLE 1. Variables and Parameters

Variables/Parameters	(Initial) Value	Reference
T	Uninfected CD4 ⁺ T cells	10^6 ml^{-1}
I_s	CD4 ⁺ T cells actively infected by wild-type virions	0
L_s	CD4 ⁺ T cells latently infected by wild-type virions	0
V_s	Wild-type HIV virions	10^{-6} ml^{-1}
I_r	CD4 ⁺ T cells actively infected by mutated virions	0
L_r	CD4 ⁺ T cells latently infected by mutated virions	0
V_r	Mutated/Drug-resistant HIV population size	0
λ	Rate of supply of immunocompetent CD4 ⁺ T cells	$10^4 \text{ ml}^{-1} \text{ day}^{-1}$
d_T	Death rate of uninfected T cells	0.01 day^{-1}
k_s	Infection rate of T cells by wild-type HIV	$2.4 \times 10^{-8} \text{ ml day}^{-1}$
k_r	Infection rate of T cells by mutated HIV	$2.0 \times 10^{-8} \text{ ml day}^{-1}$
p	Rate of latent infection in T cell population	0.1
d_I	Death rate of actively infected T cells	1 day^{-1}
d_L	Death rate of latently infected T cells	$4 \times 10^{-3} \text{ day}^{-1}$
α_s	Activation rate for latently infected wild-type T cells	0.01
α_r	Activation rate for latently infected mutated T cells	0.01
N_s	Burst size of wild-type virus	3000
N_r	Burst size of mutated/drug-resistant virus	2000
μ	Mutation rate from wild-type to mutated	3×10^{-5}
d_V	Clearance rate of free virus	23 day^{-1}

of (7CM) as $t \rightarrow \infty$. A number of long calculations show that exactly three steady states exist - E_0 , E_r and E_c , given by

$$\mathbf{E}_0 = \begin{pmatrix} \frac{\lambda}{d_T} \\ 0 \\ 0 \\ 0 \\ 0 \\ 0 \end{pmatrix}, \quad \mathbf{E}_r = \begin{pmatrix} \frac{\lambda}{d_T R_r} \\ 0 \\ 0 \\ 0 \\ \frac{d_T d_V}{k_r N_r d_I} (R_r - 1) \\ \frac{\lambda p}{R_r (d_L + \alpha_r)} (R_r - 1) \\ \frac{d_T}{k_r} (R_r - 1) \end{pmatrix}, \quad \mathbf{E}_c = \begin{pmatrix} \frac{\lambda}{d_T R_c} \\ \frac{d_T d_V (\sigma_c - 1)}{d_I k_s N_s (1-\mu)(\sigma-1)} (R_c - 1) \\ \frac{\lambda p (\sigma_c - 1)}{R_s (d_L + \alpha_s) (1-\mu)(\sigma-1)} (R_c - 1) \\ \frac{d_T (\sigma_c - 1)}{k_s (1-\mu)(\sigma-1)} (R_c - 1) \\ \frac{\mu d_T d_V}{d_I k_r N_r (1-\mu)(\sigma-1)} (R_c - 1) \\ \frac{\mu \lambda p}{R_r (d_L + \alpha_r) (1-\mu)(\sigma-1)} (R_c - 1) \\ \frac{\mu d_T}{k_r (1-\mu)(\sigma-1)} (R_c - 1) \end{pmatrix}$$

where the newly-introduced parameters R_r , R_s , R_c , σ and σ_c are defined as

$$R_r = \frac{\lambda k_r N_r (\alpha_r + (1-p)d_L)}{d_T d_V (d_L + \alpha_r)}, \quad R_s = \frac{\lambda k_s N_s (\alpha_s + (1-p)d_L)}{d_T d_V (d_L + \alpha_s)} \\ R_c = (1-\mu)R_s, \quad \sigma = \frac{R_s}{R_r}, \quad \sigma_c = (1-\mu)\sigma.$$

E_0 is the infection-free steady state, in which all populations but T are zero. Within E_r , the mutation dominant steady state, only the mutated strain remains present as I_s , L_s and V_s are zero. E_c is the state in which both strains

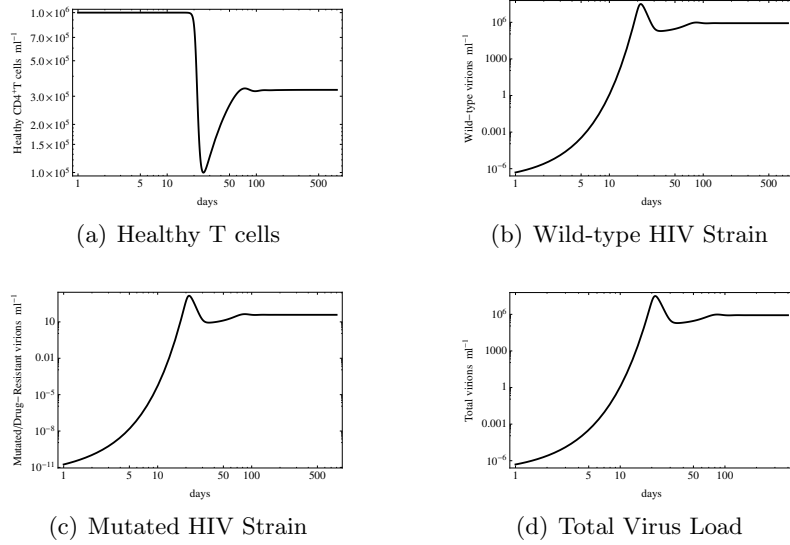


FIGURE 1. A log-log simulation of (7CM) with parameters given in Table 1. Notice that the wild-type viral strain is dominant.

persist, and hence is referred to as the coexistence steady state. To represent biological quantities, all steady state components must be nonnegative. Clearly, this is the case for E_0 . Since all parameters are positive, we see that $R_r > 1$ implies that E_r satisfies this requirement. Similarly, E_c requires $R_c > 1$ and $\sigma_c > 1$, which implies $R_s > \frac{1}{(1-\mu)}$ and $R_s > \frac{1}{(1-\mu)}R_r$. Note that $\sigma_c > 1$ implies $\sigma > 1$. Fig. 2 displays the regions in the (R_r, R_s) -plane for which steady states are nonnegative.

Finally, we wish to determine whether such states correspond to locally asymptotically stable (l.a.s) or unstable equilibria. In this vein, we prove

Theorem 1. *The stability properties of the equilibria depend only upon the two parameters R_r and R_s . Moreover,*

1. *The infection-free steady state E_0 is l.a.s. if and only if*

$$R_s < 1/(1 - \mu) \text{ and } R_r < 1,$$

and it is unstable otherwise.

2. *The steady state with only the mutated virus, E_r is l.a.s. if and only if*

$$R_s < R_r/(1 - \mu) \text{ and } R_r > 1,$$

and it is unstable otherwise.

3. *The coexistence steady state E_c is l.a.s. if and only if*

$$R_s > 1/(1 - \mu) \text{ and } R_s > R_r/(1 - \mu),$$

and it is unstable otherwise.

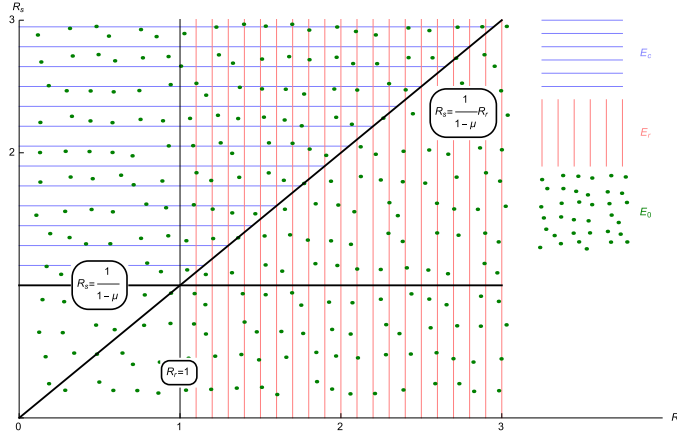


FIGURE 2. Regions of biologically-relevant existence for steady states in the (R_r, R_s) -plane.

Proof. As in [3, 7] we consider the linearization of the system to justify conclusions about its local asymptotic behavior. To begin, we consider the state E_0 , and evaluate the Jacobian of the system at this point. In particular, we are interested in the eigenvalues of the matrix

$$\nabla \mathbf{f}(\mathbf{E}_0) = \begin{pmatrix} -d_T & 0 & 0 & -\frac{\lambda k_s}{d_T} & 0 & 0 & -\frac{\lambda k_r}{d_T} \\ 0 & -d_I & \alpha_s & \frac{(p-1)\lambda(\mu-1)k_s}{d_T} & 0 & 0 & 0 \\ 0 & 0 & -d_L - \alpha_s & -\frac{p\lambda(\mu-1)k_s}{d_T} & 0 & 0 & 0 \\ 0 & d_I N_s & 0 & -d_V & 0 & 0 & 0 \\ 0 & 0 & 0 & -\frac{(p-1)\lambda\mu k_s}{d_T} & -d_I & \alpha_r & -\frac{(p-1)\lambda k_r}{d_T} \\ 0 & 0 & 0 & \frac{p\lambda\mu k_s}{d_T} & 0 & -d_L - \alpha_r & \frac{p\lambda k_r}{d_T} \\ 0 & 0 & 0 & 0 & d_I N_r & 0 & -d_V \end{pmatrix}.$$

The seven eigenvalues are $\lambda_1 = -d_T$; $\lambda_{2,3,4}$ defined by the roots of the cubic

$$a_3 x^3 + a_2 x^2 + a_1 x + a_0$$

where $a_3 = 1$ and $a_2 = d_I d_T + d_L d_T + \alpha_r d_T + d_T d_V$ are both positive, and

$$a_1 = d_T^2(d_V + d_I)(d_L + \alpha_r) + d_T^2 d_V d_I - d_T d_I(1-p)\lambda k_r N_r,$$

$$a_0 = d_T^3 d_V d_I (d_L + \alpha_r) - d_I d_T^2 \lambda k_r N_r (\alpha_r + (1-p)d_L)$$

and $\lambda_{5,6,7}$ defined as the roots of the cubic polynomial

$$b_3 x^3 + b_2 x^2 + b_1 x + b_0$$

where $b_3 = 1$ and $b_2 = d_I d_T + d_L d_T + \alpha_s d_T + d_T d_V$ are both positive, and

$$b_1 = d_T^2(d_V + d_I)(d_L + \alpha_s) + d_T^2 d_V d_I - d_T d_I(1-\mu)(1-p)\lambda k_s N_s,$$

$$b_0 = d_T^3 d_V d_I (d_L + \alpha_s) - d_T^2 d_I (1-\mu)\lambda k_s N_s (\alpha_s + (1-p)d_L).$$

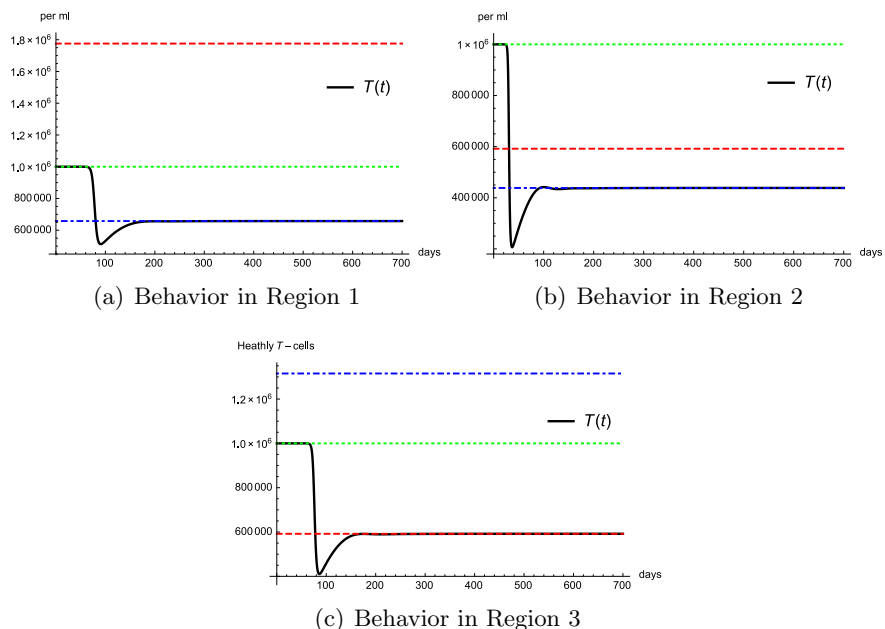
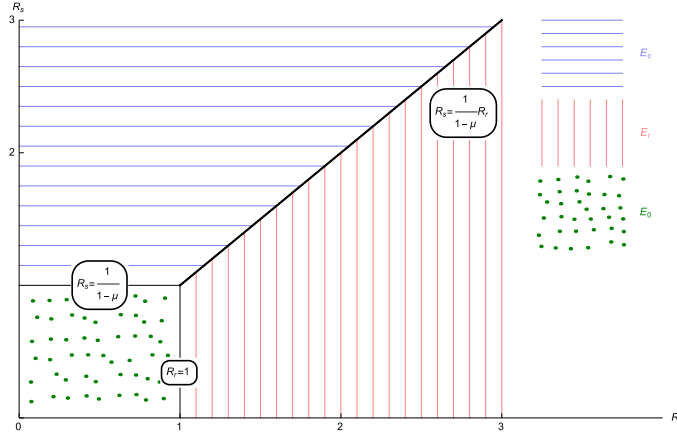


FIGURE 3. Stability of steady states in various regions of the (R_r, R_s) -plane. In each figure, the T component of E_0 , E_r , and E_c is represented by dotted, dashed, and dot-dashed lines, respectively, while the solid curve is the solution $T(t)$ with $T(0) = 10^6$.

It follows from the Hartman-Grobman Theorem that E_0 is l.a.s if and only if $\text{Re}(\lambda_i) < 0$ for all eigenvalues, λ_i , of $\nabla f(E_0)$. By the Routh-Hurwitz Theorem, the roots of the cubics possess negative real parts if and only if $a_0, a_1, a_2, a_3 > 0$ and $a_2a_1 > a_3a_0$. Clearly, $a_2, a_3, b_2, b_3 > 0$. For the first cubic, $a_1, a_0 > 0$ and $a_2a_1 > a_0$ are satisfied for $R_r < 1$. For the second cubic, the corresponding requirements are satisfied if and only if $R_s < \frac{1}{1-\mu}$. Hence, E_0 is l.a.s for the specified conditions. A similar analysis proves the second and third conclusions of the theorem. For brevity, we omit the details but take a computational approach to demonstrate their validity.

Fig. 2 displays the regions in which nonnegative steady states exist. In the area of the (R_r, R_s) -plane where $R_s > \frac{1}{1-\mu}$ and $R_r < 1$ (Region 1), both E_0 and E_c exist. For $R_s > \frac{1}{1-\mu}R_r$ and $R_r > 1$ (Region 2), all three steady states exist. For $R_s < \frac{1}{1-\mu}R_r$ and $R_r > 1$ (Region 3), both E_0 and E_r exist. Simulations are used to demonstrate the stability of coexisting states. We first begin with parameter values placing (R_r, R_s) in Region 1. Note in Fig. 3(a) that $T(t)$ (solid) tends to the corresponding value of E_c (dot-dashed). Next, (R_r, R_s) is adjusted to lie within Region 2, in which all steady states exist. Fig. 3(b) shows that $T(t)$ still tends to the corresponding value in E_c . Thus, simulations validate the results of the theorem, namely that within Regions 1 and 2, E_c is l.a.s. while E_0 and E_r are unstable. Using (R_r, R_s) within Region 3, Fig. 3(c) demonstrates that $T(t)$ tends

FIGURE 4. Regions of stability of equilibrium points in the (R_r, R_s) -plane

to the corresponding value of E_r (dashed) as $t \rightarrow \infty$. Thus in Region 3, E_r is l.a.s. While only the healthy T cell population is shown, all other populations display the corresponding long term behavior. These findings and the theorem are summarized by Fig. 4. \square

3. Drug Therapy. In the previous section it was shown that the long term behavior of (7CM) depends crucially upon parameter values, and even in the presence of viral mutation, the virus may be completely cleared from the body. Contrastingly, the mutated strain may dominate the dynamics, which can lead to drug resistance. Next, we consider the introduction of antiretroviral therapy (ART), specifically reverse transcriptase inhibitors (RTIs). These drugs hinder the replication process and decrease the rate of infection, thus altering k_s and k_r . Let ε_s represent the efficacy rate of the RTI on the wild strain. We assume the RTI combats this strain, while the mutated strain is more resistant to the drug. Hence, the efficacy of the RTI on the drug resistant strain is given by $\varepsilon_r = \alpha \varepsilon_s$, where $\alpha \in (0, 1)$ represents the resistance level. Note that smaller values of α correspond to greater levels of resistance. Including ART within the previous model yields:

$$\left. \begin{aligned} \frac{dT}{dt} &= \lambda - d_T T - (1 - \varepsilon_s)k_s T V_s - (1 - \varepsilon_r)k_r T V_r \\ \frac{dL_s}{dt} &= (1 - p)(1 - \mu)(1 - \varepsilon_s)k_s T V_s + \alpha_s L_s - d_I I_s \\ \frac{dL_r}{dt} &= p(1 - \mu)(1 - \varepsilon_s)k_s T V_s - \alpha_r L_r - d_L L_s \\ \frac{dV_s}{dt} &= N_s d_I I_s - d_V V_s \\ \frac{dI_r}{dt} &= (1 - p)\mu(1 - \varepsilon_s)k_s T V_s + (1 - p)(1 - \varepsilon_r)k_r T V_r + \alpha_r L_r - d_I I_r \\ \frac{dL_r}{dt} &= p\mu(1 - \varepsilon_s)k_s T V_s + p(1 - \varepsilon_r)k_r T V_r - \alpha_r L_r - d_L L_r \\ \frac{dV_r}{dt} &= N_r d_I I_r - d_V V_r. \end{aligned} \right\} \quad (7CM_\varepsilon)$$

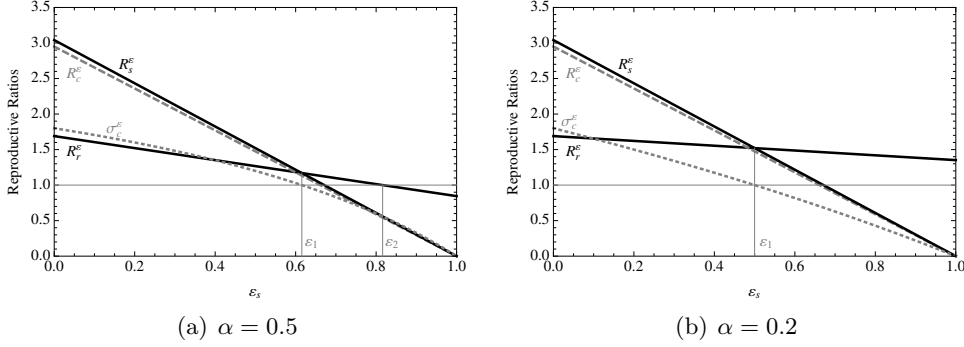


FIGURE 5. For visual clarification the difference between R_s^ε and R_c^ε has been enlarged by taking $\mu = 3 \times 10^{-2}$ in R_c^ε . Note the threshold differences between $\alpha = 0.5$ (left) and $\alpha = 0.2$ (right).

Based on similarities between (7CM) and (7CM $_\varepsilon$), the steady states are merely E_0 , E_r , and E_c under the transformations $k_s \mapsto (1 - \varepsilon_s)k_s$ and $k_r \mapsto (1 - \varepsilon_r)k_r$. We denote them by E_0^ε , E_r^ε , and E_c^ε , respectively. The new parameters R_r^ε and R_s^ε (as well as R_c^ε , σ_c^ε and σ_r^ε) are defined similarly:

$$R_r^\varepsilon = (1 - \varepsilon_r)R_r, \quad R_s^\varepsilon = (1 - \varepsilon_s)R_s.$$

Hence, the stability properties can be deduced from Theorem 1 by substituting $R_r = R_r^\varepsilon$, and $R_s = R_s^\varepsilon$.

We examine how the reproductive ratios are affected by ART for increasing drug efficacy rates assuming a particular resistance level, in this case $\alpha = 0.5$. In Fig. 5(a), the efficacy rate ε_s is plotted against reproductive ratios, R_s^ε and R_r^ε , along with R_c^ε and σ_c^ε to view changes in long term behavior. The threshold values constituting these changes are denoted by ε_1 and ε_2 . For values of $\varepsilon_s < \varepsilon_1$, we observe $R_c^\varepsilon > 1 \Leftrightarrow R_s^\varepsilon > \frac{1}{1-\mu}$ and $\sigma_c^\varepsilon > 1 \Leftrightarrow R_s^\varepsilon > \frac{1}{1-\mu} R_r^\varepsilon$. Thus by Theorem 1, we conclude that solutions tend to E_c^ε . Contrastingly, for $\varepsilon_1 < \varepsilon_s < \varepsilon_2$, $R_r^\varepsilon > 1$ and $\sigma_c^\varepsilon < 1$ thus solutions tend to E_r^ε . It is not until $\varepsilon_s > \varepsilon_2$, when $R_r^\varepsilon < 1$ and $R_c^\varepsilon < 1$, that the efficacy is large enough to force viral clearance.

To investigate the change in the long term behavior of the viral loads, we graph the steady state values of V_r and V_s separately against ε_s . Figs. 6(a) and 6(b) display the change in the drug resistant virus population. Fig. 6(a) shows the dramatic increase in the drug resistant population near $\varepsilon_s = \varepsilon_1$, but this scale cannot accurately display values for $\varepsilon_s < \varepsilon_1$. Thus Fig. 6(b), an enlargement, shows the slow increase in this population. In Fig. 6(c), we note the steady decline in the wild population as ε_s increases and its extinction at $\varepsilon_s = \varepsilon_1$. Fig. 6(d) displays the total virus population.

The question arises whether a value of α exists which prohibits viral clearance altogether. A higher resistance level of the mutated strain is chosen, and the steady state behavior is examined. Fig. 5(b) shows the reproduction numbers assuming $\alpha = 0.2$. The threshold $\varepsilon_1 = 0.5$ when $\sigma_c^\varepsilon = 1$ indicates

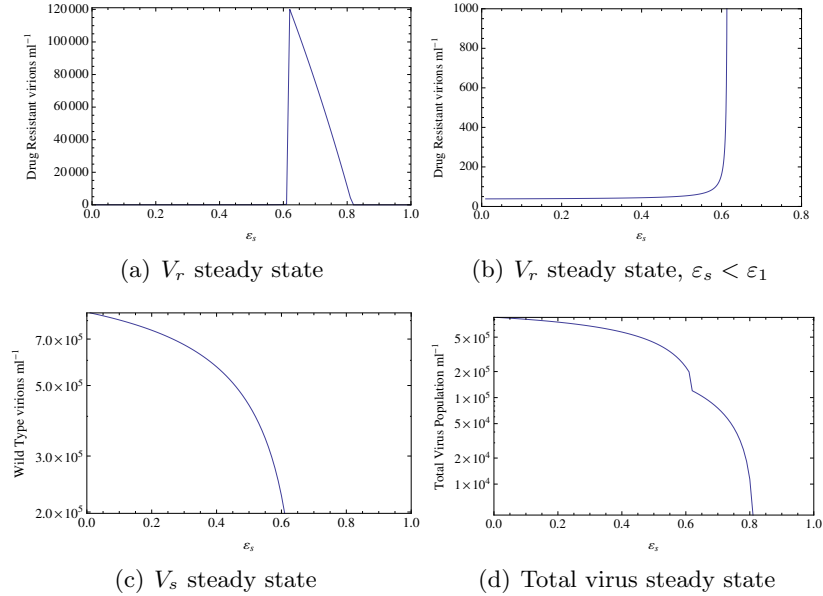


FIGURE 6. Steady state values for both wild type and drug resistant virus population with respect to ε_s , assuming $\alpha = 0.5$.

the shift from the coexistent state to drug resistant dominance. There is no longer an ε_2 threshold, which implies that no drug efficacy could be large enough to counter the resistance level of the mutant strain. Thus, the RTI would clear only the wild type virus. Fig. 7(a) demonstrates that even when $\varepsilon_s = 1$, the resistant steady state remains prohibitive. In Fig. 7(c), we note the faster decline in the wild population as ε_s increases and the earlier extinction at ε_1 as compared to Fig. 6(c). Fig. 7(d) displays the total virus population, demonstrating continued viral persistence as $\varepsilon_s \rightarrow 1$, unlike Fig. 6(d). Therefore, viral mutation and drug resistance can completely inhibit the treatment ability of RTIs.

4. Conclusions. Upon formulating a new in-host model of HIV dynamics that incorporates latent infection and viral mutation, the local asymptotic behavior of the model was characterized and validated using computational means. The effects of RTIs were elucidated under differing drug resistance levels for the mutated strain. In particular, our analysis determined that a sufficiently high resistance level arising from viral mutation could render a persistent infection untreatable. This implies that RTIs alone are not strong enough to counteract the emergence of drug resistant strains. Additionally, as HIV possesses a strong propensity to mutate, due to common errors in reverse transcription, the effects of viral mutation are significant within the dynamics of the virus.

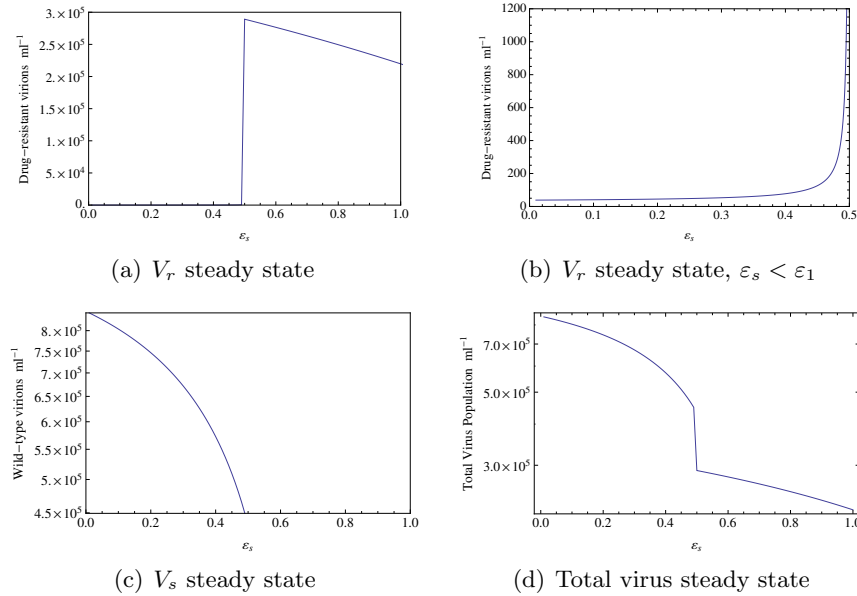


FIGURE 7. Dynamics of steady states for wild type and drug resistant virions with respect to drug efficacy, assuming $\alpha = 0.2$.

REFERENCES

- [1] M. Nowak and R. May, *Virus Dynamics: Mathematical Principles of Immunology and Virology*, Oxford University Press (2000), ISBN: 9780198504177.
- [2] S. Pankavich, The effects of latent infection on the dynamics of HIV, *Differential Equations and Dynamical Systems* (2015), doi: 10.1007/s12591-014-0234-6.
- [3] C. Parkinson and S. Pankavich, Mathematical Analysis of an in-host Model of Viral Dynamics with Spatial Heterogeneity, *submitted*.
- [4] A. Perelson, D. Kirschner, and R. Boer, Dynamics of HIV Infection of CD4⁺ T cells, *Math. Biosci.* **114** (1993) 81-125.
- [5] A. Perelson and P. Nelson, Mathematical analysis of HIV-1 dynamics in vivo, *SIAM Review*, **41** (1999), 3–44.
- [6] A. Perelson and R. Ribeiro, Modeling the within-host dynamics of HIV infection, *BMC Biology*, **11** (2013), 96.
- [7] P. Roemer, E. Jones, M. Raghupathi, and S. Pankavich, Analysis and Simulation of the three-component model of HIV dynamics, *SIAM Undergraduate Research Online*, **7** (2014) 89-106.
- [8] L. Rong, Z. Feng, and A. Perelson, Emergence of HIV-1 drug resistance during anti-retroviral treatment, *Bull. Math. Biol.*, **69** (2007), 2027–2060.
- [9] L. Rong and A. Perelson, Modeling HIV persistence, the latent reservoir, and viral blips, *Journal of Theoretical Biology* **260** (2009), 308-331.
- [10] L. Rong and A. Perelson, Modeling Latently Infected Cell Activation: Viral and Latent Reservoir Persistence, and Viral Blips in HIV-infected Patients on Potent Therapy, *PLoS Computational Biology* **5** (2009), doi: 10.1371/journal.pcbi.1000533.
- [11] R. Shonkwiler and J. Herod, An Introduction with Maple and Matlab, in *Undergraduate Texts in Mathematics: Mathematical Biology*, Springer, New York, (2009).

E-mail address: pankavic@mines.edu

E-mail address: dshutt@mines.edu